Geochemical Perspectives Letters

Magnetic foraminifera thrive in the Mariana Trench

H. Yang[1,2], X. Peng[1*], A.J. Gooday[3,4], B. Jones[5], J. Li[1], S. Liu[6], W. Huang[7], Z. Sun[8], S. Chen[1], S. Dasgupta[1], H. Xu[1], S. Liu[1], W. Xu[1], K. Ta[1]

OPEN ACCESS
https://doi.org/10.7185/geochemlet.2212

Abstract

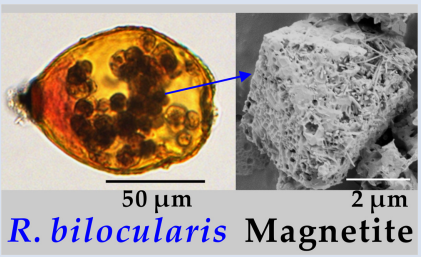

Unicellular magnetic microorganisms include magnetotactic bacteria and some protist species. Although magnetosome magnetite in bacteria (prokaryotes) is well studied, little is known regarding the characteristics and origin of magnetic minerals in protists (eukaryotes). Stercomata stored within tests of the hadal foraminifera *R. bilocularis* from the Mariana Trench (6980–10,911 m depth), contain magnetite crystals. As a result, this species can orient in accordance with magnetic fields. The magnetite differs chemically and physically from that in the surrounding sediments. The crystals also differ from bacterial magnetosomes in being of variable size, porous structure, not arranged in chains, and encapsulated in a lipid membrane. Putting available evidence together indicates a biological origin of the magnetite, although a sedimentary source cannot be eliminated. This is the first record of a magnetic protist from hadal depths, opening a new window for the biomagnetism in the Earth's extreme environment.

Received 24 November 2021 | Accepted 25 March 2022 | Published 20 April 2022

Introduction

Biogenic magnetite occurs inside magnetotactic bacteria (Mann *et al.*, 1984) and some protists (algae and protozoa) (Bazylinski *et al.*, 2012; Leão *et al.*, 2020; Monteil and Lefevre, 2020), the latter including a number of biflagellates, dinoflagellates, and ciliates, as well as multicellular animals (insects, molluscs, fish, birds, and mammals) (Frankel, 1984; Kirschvink *et al.*, 2001). In these organisms, magnetite facilitates magnetic field detection, making it possible for them to orientate and navigate (Maugh, 1982; Andrews *et al.*, 2003). Bacteria and protists are particularly important in this regard, because their simple structure and wide distribution in various aquatic environments facilitates the study of biogenic magnetite formation and magnetotaxis (Bazylinski and Frankel, 2004; Bazylinski *et al.*, 2012; Leão *et al.*, 2020). Although the synthesis of magnetite nanoparticles in magnetotactic bacteria is well studied (Uebe and Schüler, 2016), the formation mechanisms of magnetite and its physiological functions in eukaryotic protists remain largely unknown.

Several protistan taxa, including diplonemids, kinetoplastids, ciliates, and foraminifera (Todo *et al.*, 2005; Schoenle *et al.*, 2021), have been reported from abyssal plains and hadal trenches, where they probably play a critical role in carbon cycling (Schoenle *et al.*, 2021). Foraminifera are among the most common meiofauna-sized organisms at hadal depths greater than 6000 m. Between 2016 and 2019, exploration by the R/V *TANSUOYIHAO* (Table S-1) at 11 stations in the southern Mariana Trench at water depths between 6980 and 10,911 m, recovered numerous specimens of the organic walled species *R. bilocularis* from the surface sediments. This species, which had been described earlier from the Mariana Trench (Gooday *et al.*, 2008) and is currently classified within the foraminiferal class Monothalamea ('monothalamids'), was found to be highly magnetic (Fig. 1a,b).

Results

Response of foraminifera to magnetic fields. All *R. bilocularis* specimens in a sample of 1000 observed in this study showed varying degrees of passive response to the applied magnetic field (Video S-1). A magnetite enrichment experiment based on 1000 *R. bilocularis* showed that each specimen contained an average of 1020 ng of magnetite. Analyses of the single cell magnetic dipole moment of 31 *R. bilocularis* using a miniaturised atomic magnetometer revealed that their magnetic response is based on a permanent magnetic dipole moment (M) *per* cell, which ranged from 1.10×10^{-14} to 1.51×10^{-11} J/T. The ratio of magnetic to thermal energy, MB/k_BT, calculated from the average upper limit

1. Laboratory of Deep-Sea Geology and Geochemistry, Institute of Deep-Sea Science and Engineering, Chinese Academy of Sciences, Sanya, 572000, China
2. University of Chinese Academy of Sciences, Chinese Academy of Sciences, Beijing, 100049, China
3. National Oceanography Centre, European Way, Southampton SO14 3ZH, UK
4. Life Sciences Department, Natural History Museum, Cromwell Road, London SW7 5BD, UK
5. Department of Earth and Atmospheric Sciences, University of Alberta, Edmonton, Alberta T6G 2E3, Canada
6. State Key Laboratory of Lithospheric Evolution, Institute of Geology and Geophysics, Chinese Academy of Sciences, Beijing, China
7 Beijing Synchrotron Radiation Facility, Institute of High Energy Physics, Chinese Academy of Sciences, Beijing, China
8. Jiangsu Key Laboratory of Medical Optics, Suzhou Institute of Biomedical Engineering and Technology, Chinese Academy of Sciences
* Corresponding author (email: xtpeng@idsse.ac.cn)

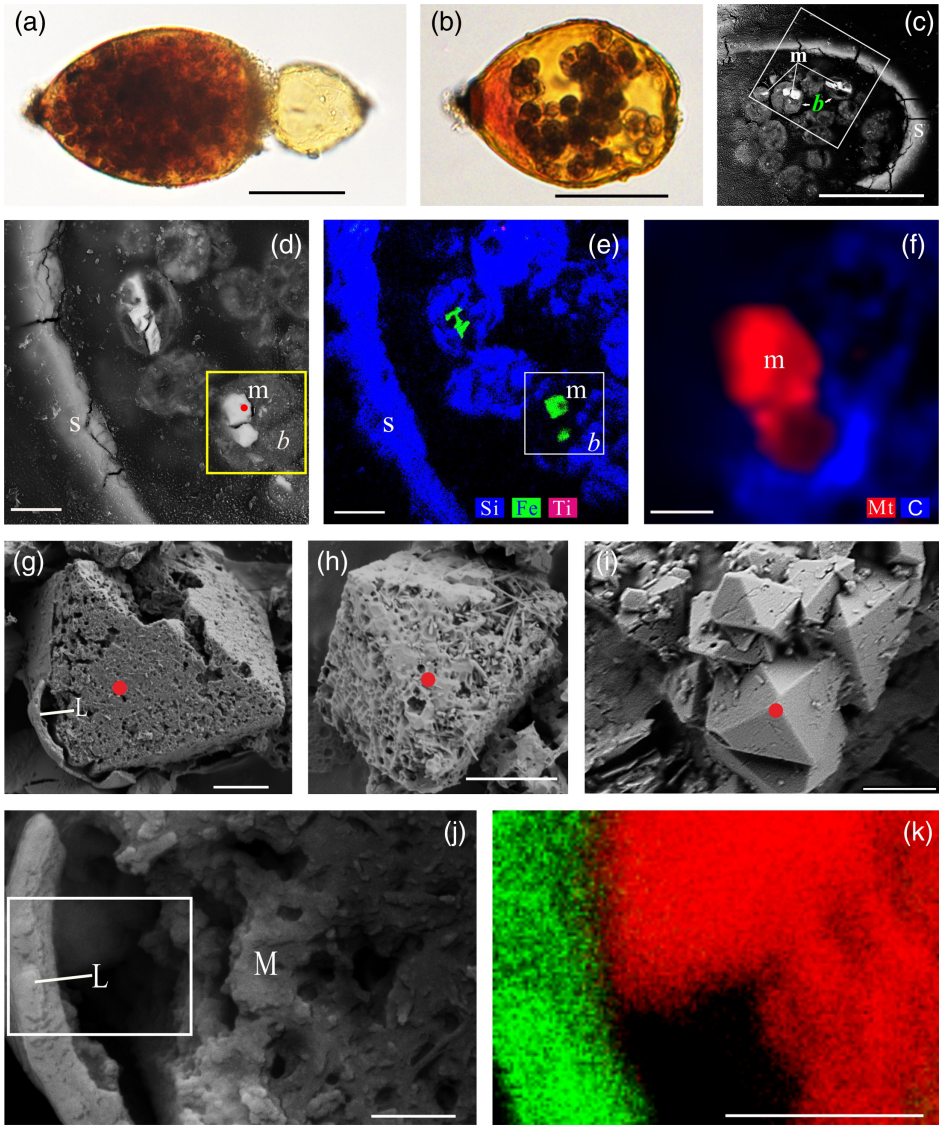

Figure 1 Magnetite in the foraminifera *R. bilocularis*. **(a)** LM (light microscopy) image showing the rusty colour of the organic walled test of *R. bilocularis* (Gooday *et al.*, 2008). **(b)** LM image of the larger chamber of *R. bilocularis* stained with Rose Bengal, with fresh stercomata (waste pellets) and stained cytoplasm concentrated just inside the aperture. **(c)** SEM image of a thin section of *R. bilocularis* from the Challenger Deep with numerous stercomata (*b*) inside the test (s). Magnetite (m) is contained in the stercomata. **(d)** Enlarged SEM image of the area indicated by the white rectangle in **(c)**. Magnetite (m) is contained in the stercomata (*b*), within the yellow box. Raman analysis position is marked with a red dot. **(e)** NanoSIMS elemental mapping of *R. bilocularis*. Blue = Si; Green = Fe; Red = Ti. SEM-EDX elemental maps are presented in Figure S-15. **(f)** Raman spectral combined images obtained from a stercome containing magnetite. Combined maps of intensity of 666 cm^{-1}, 538 cm^{-1}, 304 cm^{-1} (red) and 1367 cm^{-1}, 1582 cm^{-1} (blue), indicating magnetite and organic carbon in stercomata, respectively. **(g, h, i)** Secondary electron image of magnetite extracted from *R. bilocularis* showing a euhedral and porous structure. L = carbon-containing membrane. **(j)** An enlarged SEM image of the carbon-containing membrane enveloping the magnetite in Figure 1g. L = carbon-containing membrane, M = magnetite. **(k)** The elemental mapping of the area in white rectangular of Figure 1j. Green = carbon; Red = iron; other elements are shown in Figure S-16. Scale bars of a,b = 50 μm, c = 20 μm, d,e = 8 μm, f–i = 2 μm, j,k = 0.5 μm.

of M for the foraminifera, is 9.974×10^4 (Table S-2). The magnetic energy of *R. bilocularis* is therefore obviously much greater than the thermal energy.

Characteristics of magnetite in foraminifera. Tests of *Resigella bilocularis* contain numerous stercomata (Fig. 1a,b), waste pellets that are also present in many other hadal monothalamid foraminifera (Gooday *et al.*, 2008). Scanning electron microscopy (SEM), light microscopy and confocal laser scanning microscopy (CLSM) observations revealed multiple particles contained in the stercomata, but absent in the cytoplasm (Fig. 1c,d; Fig. S-1a,b; Fig. S-2; Fig. S-3a,b; Fig. S-4a). They are of variable size (0.15–12 μm) and not arranged in chains (Video S-2, Fig. 2c). These euhedral magnetite particles are octahedral and exhibit a porous structure (Fig. 1g–i). Secondary ion mass spectrometry (NanoSIMS) and SEM-based energy dispersive X-ray spectroscopy (EDX) revealed that they are mainly composed of Fe and O (Fig. 1e; Fig. S-4c; Fig. S-5b). Raman spectroscopy analyses further showed that they are magnetite particles (Fig. S-4b; Fig. S-6a; Fig. S-7f–h), which are commonly encapsulated by lipid membranes (Fig. 1g,j,k; Fig. 3; Fig. S-3). This is consistent with the results of synchrotron phase contrast analysis experiments showing intact porous magnetite inside stercomata (Fig. 2e; Fig. S-1e–l). The magnetic properties of the foraminifera therefore clearly originate from these micron-sized magnetite particles.

Comparison of magnetite within foraminifera with that from sediments. The magnetite crystals in the stercomata of *R.*

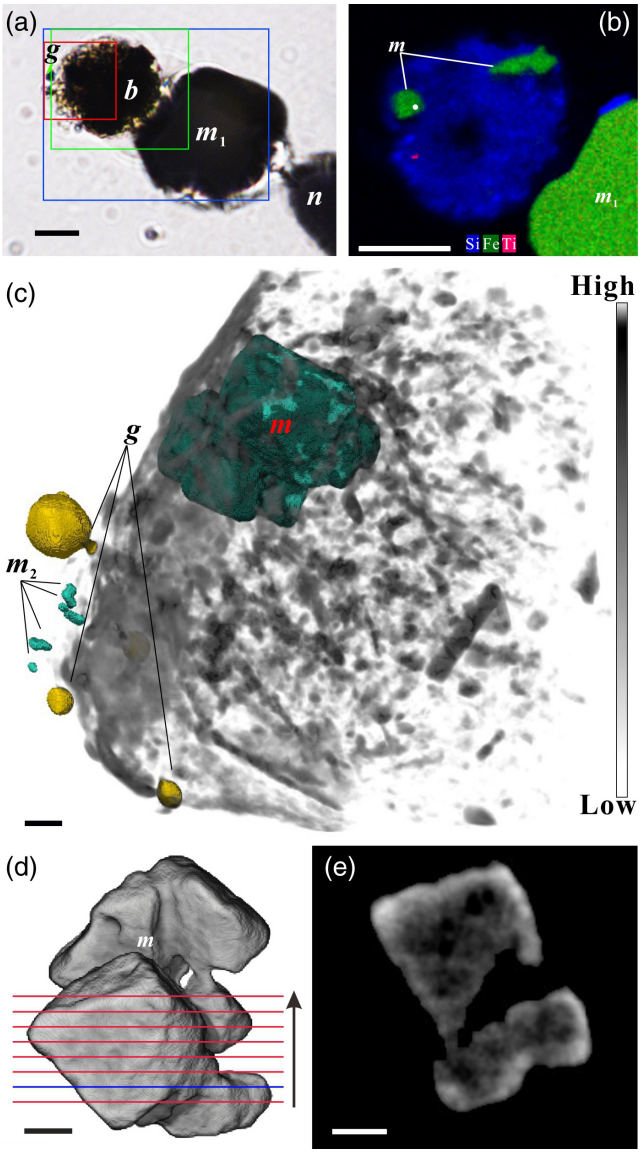

Figure 2 Synchrotron X-ray computerised tomography of a stercome from *R. bilocularis*. **(a)** Transmitted light micrograph of a stercome. The stercome (*b*) was placed on the tip of a metal needle (*n*) adhered to a titanomagnetite standard sample (m_1) and labelled with a gold particle (*g*). **(b)** The elemental distribution image characterised by SEM-EDX analysis of stercomata (green box in Fig. 2a). The stercome contains magnetite (m) and rutile (red dot location). **(c)** A phase contrast image of the foraminiferal stercome (red box range in Fig. 2a) based on synchrotron X-ray computerised tomography (NanoCT) analysis. The absorbance of the foraminiferal magnetite (*m*) is similar to that of the standard magnetite (m_2), less than that of the gold particle (*g*). **(d)** 3D reconstructions of magnetite from synchrotron X-ray computerised tomography. The same particle as that marked 'm' in Figure 2c is shown in eight cross sections from bottom to top in the direction of the arrow in Figure S-1e–l. The 3D reconstructions of the sections indicated by the red and blue lines in Figure 2d have a spatial spacing of 0.296 μm. **(e)** The 3D reconstruction of the section indicated by the blue line in Figure 2d shows the porous structure of the magnetite. Scale bars of c–e = 1 μm, others = 10 μm.

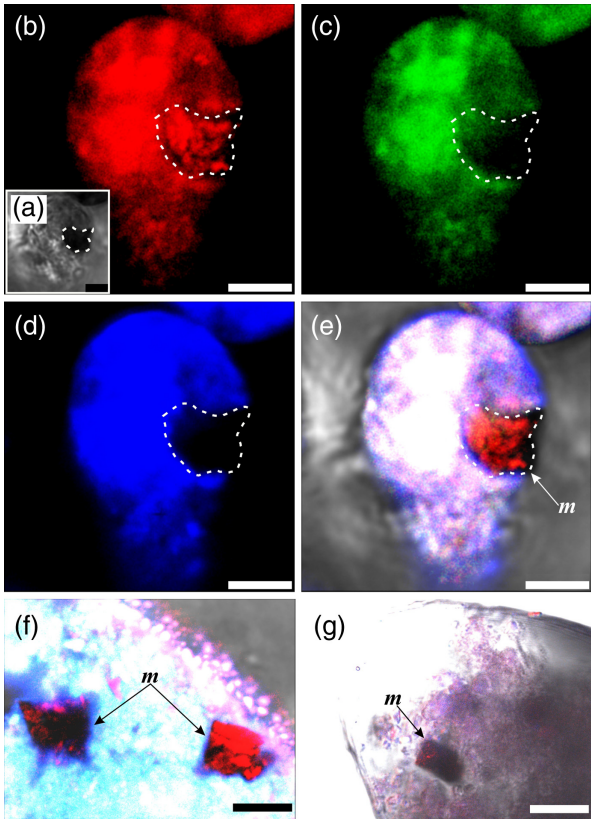

Figure 3 Magnetite (m) encrusted by lipid envelope in a stercome of *R. bilocularis*. **(a)** Reflected light micrograph of the stercome. **(b)** CLSM image of the stercome stained using Sudan IV to stain lipid shown in red. **(c)** CLSM image of the stercome stained using phalloidin to stain actin shown in green. **(d)** CLSM image of the stercome stained using DAPI to stain DNA shown in blue. **(e)** Combined image of b–d. A magnetite particle encrusted by a lipid membrane shown in red. **(f, g)** Combined images showing magnetite encrusted by a lipid membrane stained using Sudan IV. Magnetites are marked with arrow and m. Scale bars of f = 5 μm, g = 10 μm, others = 2.5 μm.

bilocularis differ in a number of respects from magnetite found in the surrounding hadal sediments. First, they commonly have an octahedral and porous structure (Fig. 1g–i), whereas magnetite in the environmental sediment has an irregular shape, smooth surfaces (Fig. S-8a) and a larger particle size (Fig. S-9; Fig. S-10). Second, magnetite particles within the foraminifera are wrapped in an organic envelope, in contrast to those from surrounding sediments, which lack this feature (Fig. 1e-k; Fig. S-3). Third, EDX analyses of magnetite particles from foraminifera demonstrated that they contain no inclusions, whereas silicate-like, magnesium oxide-like, and chrome-aluminum oxide-like inclusions are present in the magnetite from sediments, a feature shared with hydrothermal and magmatic magnetite (Ciobanu *et al.*, 2019) (Fig. S-11; Fig. S-12). Fourth, a magnetic property measurement system (MPMS) yielded a lower transition temperature (104 K) for the foraminiferal magnetite than the magnetite from sediments (111 K) (Fig. S-13).

Discussion

Origin of magnetite in R. bilocularis. The porous structure in non-biogenic magnetite generally occurs during the terrestrial weathering of magnetite to hematite (Anand and Gilkes, 1984), or as a result of the formation of magnetite during the reduction of hematite in the solid phase (Deo *et al.*, 1989). The magnetite in *R. bilocularis* did not contain any hematite that would be produced during the weathering of magnetite or left as a residue during the reduction of hematite. Hence, it is not likely that the porous structure associated with magnetite in *R. bilocularis* originates from the weathering (*i.e.* corrosion) of magnetite or the reduction of

hematite. The euhedral structure of magnetite from *R. bilocularis*, which distinctly differs from the irregular shape of magnetite from sediments, also indicates that they might have different origins. The porous structure is possibly formed due to the incorporation of organic matter into the magnetite during the formation process, as indicated by SEM-EDX analyses (Fig. S-5). The formation of minerals with porous structures due to the involvement of organic matter is also a common feature of biologically induced mineralisation (Sanz-Montero *et al.*, 2009).

The differences between the magnetite in *R. bilocularis* stercomata and the magnetite from surrounding sediments further suggests that the former may be produced within the foraminifera, as also reported for certain other protists (Leão *et al.*, 2020). Foraminiferal magnetite is encapsulated by a lipid membrane, which is also more consistent with a biogenic origin. Moreover, the relatively low transition temperature (104 K) of the foraminiferal magnetite is similar to that of biogenic magnetite produced by magnetotactic bacteria (Li *et al.*, 2010; Jackson and Bruce, 2021), perhaps providing additional indirect evidence for biogenic origin.

High throughput sequencing of *R. bilocularis* failed to reveal the presence of any associated magnetotactic bacteria, although about 0.09 % of sequences were attached to the iron reducing bacterium *Shewanella* sp. (Fig. S-14). The sequences had 94.47 % similarity with *Shewanella piezotolerans* WP3 which was isolated from deep sea sediments (Wang *et al.*, 2004). The magnetite synthesised by *S. piezotolerans* WP3 is commonly 4–8 nm in diameter and significantly smaller than that found in *R. bilocularis* (Wu *et al.*, 2013). Thus, a purely bacterial origin for the magnetite particles found in *R. bilocularis* is unlikely.

Biologically controlled mineralisation typically generates magnetite crystals with a uniform morphology, high chemical purity and arranged in chains, whereas biologically induced mineralisation (BIM) generates magnetite crystals of variable size and morphology that are not arranged in chains (Bazylinski *et al.*, 2007). The presence of a lipid membrane, together with the morphological and chemical characteristics of the *R. bilocularis* crystals, favours the hypothesis that they are most likely formed through BIM in microenvironments within stercomata, However, the collection of mineral grains is typical of foraminifera and therefore we cannot completely rule out the possibility that magnetite may be derived from surrounding sediments.

The iron reducing bacterium *Shewanella* sp. detected in *R. bilocularis* may be involved in magnetite biomineralisation within *R. bilocularis via* providing a Fe^{2+} source. We develop the following conceptual model for the formation of magnetite in foraminifera (Fig. 4). The foraminifera first feed on the iron oxides that are commonly present in the surface sediments. The semi-enclosed environment within the foraminiferal test provides conditions that permit *Shewanella* sp. to reduce Fe^{3+} in iron oxides to Fe^{2+}. Generated Fe^{2+} within the foraminiferal test then is transported into the stercomata where micron-sized magnetite is formed in the presence of organic matter (Fig. S-5a).

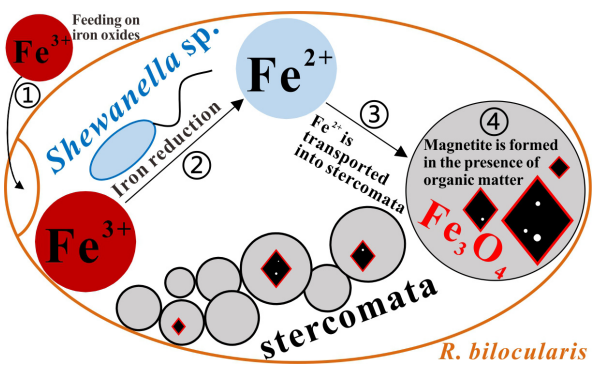

Figure 4 A conceptual model of formation of magnetite in *R. bilocularis*. 1) Foraminifera feed on sediments containing iron oxides (Fe^{3+}). 2) Reduction of Fe^{3+} to Fe^{2+} by the iron reducing bacterium *Shewanella* sp. 3) Fe^{2+} is transferred to the stercomata. 4) Formation of porous magnetite with organic matter incorporated. The red rhombs represent lipid envelopes.

Implications

Regardless of whether magnetite in *R. bilocularis* has a biological origin or is derived from surrounding sediments, their passive response to the magnetic field make them the first example of magnetic protist at hadal depths. In magnetotactic bacteria and algae, the magnetic energy is sufficient to overcome the irregular motion induced by external thermal energy, allowing these microorganisms to exhibit magnetotactic behaviour (Araujo *et al.*, 1986; Pan *et al.*, 2005). Although the magnetic energy in *R. bilocularis* is also larger than external thermal energy, this does not mean that these foraminifera must have magnetotactic capability, because larger particles, such as foraminifera 100–200 μm in size are less affected by the Brownian motion than much smaller microbial organisms (Russel, 1981). Whether the magnetite in *R. bilocularis* fulfills any physiological function remains unknown. Perhaps, these foraminifera may take advantage of the magnetite to sense the Earth's magnetic field, like some ciliates and flagellates (Monteil and Lefevre, 2020) or adjust the iron balance within the test (Andrews *et al.*, 2003). *In situ* experiments are needed to test these possibilities and better understand the origin of the magnetite crystals and other aspects of the biology of these very common but enigmatic hadal protists.

Acknowledgements

We are grateful to the crew of R/V *TANSUOYIHAO* for their hard work during the expedition (TS01 to TS14). We also appreciate the help and advice provided by Xue Liang and Yifeng Li of Shanghai University in the FIB-TEM analysis; Ye Li of the Institute of Environment and Plant Protection, Chinese Academy of Tropical Agricultural Sciences (Haikou) for her help during the production of ultrathin sections; and Jialong Hao of the Institute of Geology and Geophysics, Chinese Academy of Sciences for his help in the NanoSIMS tests. We thank Zixiao Guo of Hebei Normal University for providing detailed methods on sample preparation. We would like to thank Dong Sheng, Qianqian Yu and Siqi Liu of the University of Science and Technology of China for their guidance and assistance during the atomic magnetometer analysis. We also express our gratitude to Qingxi Yuan, Jin Zhang, Kai Zhang, Tianyu Fu and Chunxia Yao at the Beijing Synchrotron Radiation Facility (BSRF) for their help with hard X-ray phase contrast imaging and computed tomography (CT) analysis. We thank Hanna Han and her team from Shenzhen Ecogene Co., Ltd. for their technical service. We thank Zhuoli Zhao of China University of Geosciences (Beijing) for the data processing of 16S high-throughput sequencing. This study was financially supported by the National Key Research and Development Program of China (Grant No. 2016YFC0304900). We thank two anonymous reviewers for their comments which led to substantial improvements in the manuscript.

Editor: Juan Liu

Additional Information

Supplementary Information accompanies this letter at http://doi.org/10.7185/geochemlet.2212.

Cite this letter as: Yang, H., Peng, X., Gooday, A.J., Jones, B., Li, J., Liu, S., Huang, W., Sun, Z., Chen, S., Dasgupta, S., Xu, H., Liu, S., Xu, W., Ta, K. (2022) Magnetic foraminifera thrive in the Mariana Trench. *Geochem. Persp. Let.* 21, 23–27. https://doi.org/10.7185/geochemlet.2212

References

Anand, R.R., Gilkes, R.J. (1984) Mineralogical and chemical properties of weathered magnetite grains from lateritic saprolite. *European Journal of Soil Science* 35, 559–567. https://doi.org/10.1111/j.1365-2389.1984.tb00613.x

Andrews, S.C., Robinson, A.K., Rodríguez-Quiñones, F. (2003) Bacterial iron homeostasis. *FEMS Microbiology Reviews* 27, 215–237. https://doi.org/10.1016/S0168-6445(03)00055-X

Araujo, F.D., Pires, M.A., Frankel, R.B., Bicudo, C. (1986) Magnetite and magnetotaxis in algae. *Biophysical Journal* 50, 375–378. https://doi.org/10.1016/S0006-3495(86)83471-3

Bazylinski, D.A., Frankel, R.B. (2004) Magnetosome formation in prokaryotes. *Nature Reviews Microbiology* 2, 217–230. https://doi.org/10.1038/nrmicro842

Bazylinski, D.A., Frankel, R.B., Konhauser, K.O. (2007) Modes of biomineralization of magnetite by microbes. *Geomicrobiology Journal* 24, 465–475. https://doi.org/10.1080/01490450701572259

Bazylinski, D.A., Lefèvre, C.T., Frankel, R.B. (2012) Magnetotactic protists at the oxic–anoxic transition zones of coastal aquatic environments. *Anoxia* 21, 131–143. https://doi.org/10.1007/978-94-007-1896-8_7

Ciobanu, C.L., Verdugo-Ihl, M.R., Slattery, A., Cook, N.J., Ehrig, K., Courtney-Davies, L., Wade, B.P. (2019) Silician magnetite: Si–Fe-nanoprecipitates and other mineral inclusions in magnetite from the Olympic Dam Deposit, South Australia. *Minerals* 9, 311–346. https://doi.org/10.3390/min9050311

Deo, B., Dube, R.K., Chatterji, S. (1989) Formation of porous magnetite in the initial stages of solid state reduction of hematite by metallic iron. *ISIJ International* 29, 345–347. https://doi.org/10.2355/isijinternational.29.345

Frankel, R.B. (1984) Magnetic Guidance of Organisms. *Annual Review of Biophysics and Bioengineering* 13, 85–103. https://doi.org/10.1146/annurev.bb.13.060184.000505

Gooday, A.J., Todo, Y., Uematsu, K., Kitazato, H. (2008) New organic-walled Foraminifera (Protista) from the ocean's deepest point, the Challenger Deep (western Pacific Ocean). *Zoological Journal of the Linnean Society* 3, 399–423. https://doi.org/10.1111/j.1096-3642.2008.00393.x

Jackson, M.J., Bruce, M. (2021) On the distribution of Verwey transition temperatures in natural magnetites. *Geophysical Journal International* 2, 1314–1325. https://doi.org/10.1093/gji/ggaa516

Kirschvink, J.L., Walker, M.M., Diebel, C.E. (2001) Magnetite-based magnetoreception. *Current Opinion in Neurobiology* 11, 462–467. https://doi.org/10.1016/S0959-4388(00)00235-X

Li, J.H., Pan, Y.X., Liu, Q.S., Qin, H.F., Deng, C.L., Che, R.C., Yang, X.A. (2010) A comparative study of magnetic properties between whole cells and isolated magnetosomes of magnetospirillum magneticum AMB-1. *Chinese Science Bulletin* 55, 38–44. https://doi.org/10.1007/s11434-009-0333-x

Leão, P., Le Nagard, L., Yuan, H., Cypriano, J., Da Silva-Neto, I., Bazylinski, D.A., Acosta-Avalos, D., Barros, H.L., Hitchcock, A.P., Lins, U., Abreu, F. (2020) Magnetosome magnetite biomineralization in a flagellated protist: evidence for an early evolutionary origin for magnetoreception in eukaryotes. *Environmental Microbiology* 22, 1495–1506. https://doi.org/10.1111/1462-2920.14711

Mann, S., Frankel, R.B., Blakemore, R.P. (1984) Structure, morphology and crystal growth of bacterial magnetite. *Nature* 310, 405–407. https://doi.org/10.1038/310405a0

Maugh, T. (1982) Magnetic navigation an attractive possibility. *Science* 215, 1492–1493. https://doi.org/10.1126/science.7063857

Monteil, C.L., Lefevre, C.T. (2020) Magnetoreception in Microorganisms. *Trends in Microbiology* 28, 266–275. https://doi.org/10.1016/j.tim.2019.10.012

Pan, Y., Petersen, N., Davila, A.F., Zhang, L.M., Winklhofer, M., Liu, Q.S., Hanzlik, M., Zhu, R.X. (2005) The detection of bacterial magnetite in recent sediments of Lake Chiemsee (southern Germany). *Earth and Planetary Science Letters* 232, 109–123. https://doi.org/10.1016/j.epsl.2005.01.006

Russel, W.B. (1981) Brownian motion of small particles suspended in liquids. *Annual Review of Fluid Mechanics* 13, 425–455. https://doi.org/10.1146/annurev.fl.13.010181.002233

Sanz-Montero, M.E., Rodríguez-Aranda, J.P., Cura, M. (2009) Bioinduced precipitation of barite and celestite in dolomite microbialites: Examples from Miocene lacustrine sequences in the Madrid and Duero Basins, Spain. *Sedimentary Geology* 222, 138–148. https://doi.org/10.1016/j.sedgeo.2009.05.009

Schoenle, A., Hohlfeld, M., Hermanns, K., Mahe, F., Vargas, C.D., Nitsche, F., Arndt, H. (2021) High and specific diversity of protists in the deep-sea basins dominated by diplonemids, kinetoplastids, ciliates and foraminiferans. *Communications Biology* 4, 501–511. https://doi.org/10.1038/s42003-021-02012-5

Todo, Y., Kitazato, H., Hashimoto, J., Gooday, A.J. (2005) Simple foraminifera flourish at the ocean's deepest point. *Science* 307, 689–689. https://doi.org/10.1126/science.1105407

Uebe, R., Schüler, D. (2016) Magnetosome biogenesis in magnetotactic bacteria. *Nature Reviews Microbiology* 14, 621–637. https://doi.org/10.1038/nrmicro.2016.99

Wang, F.P., Wang, P., Chen, M.X., Xiao, X. (2004) Isolation of extremophiles with the detection and retrieval of Shewanella strains in deep-sea sediments from the west Pacific. *Extremophiles* 8, 165–168. https://doi.org/10.1007/s00792-003-0365-0

Wu, W.F., Wang, F.P., Li, J.H., Yang, X.M., Pan, Y.X. (2013) Iron reduction and mineralization of deep-sea iron reducing bacterium Shewanella piezotolerans WP3 at elevated hydrostatic pressures. *Geobiology* 11, 593–601. https://doi.org/10.1111/gbi.12061